Advanced Journal of Vascular Medicine

Research Article

Characteristics of Arterial Wall Stiffness in Healthy Adolescents: Preliminary Mechanical Mapping of the Main Upper Body Arterial Branches - ∂

Roch L. Maurice[1,2]*, Katherine YH. Chen[3,4], David Burgner[3,4,5], Michael Cheung[3], Laurence Vaujois[1], Anne-Monique Nuyt[2,6], Jean-Luc Bigras[1,2], and Nagib Dahdah[1,2]

[1]Division de la Cardiologie Pédiatrique, Centre Hospitalier Universitaire Sainte Justine (CHUSJ), Université de Montréal, Montréal, QC, Canada

[2]Centre de Recherche, Centre Hospitalier Universitaire Sainte Justine (CRCHUSJ), Université de Montréal, Montréal, QC, Canada

[3]Murdoch Childrens Research Institute, Parkville, Victoria, Australia

[4]Department of Paediatrics, University of Melbourne, Parkville, Victoria, Australia

[5]Department of Paediatrics, Monash University, Clayton, Victoria, Australia

[6]Neonatal Service, CHUSJ, Montreal University, Montréal, Canada

***Address for Correspondence:** Roch L. Maurice, Centre de Recherche, CHU Sainte Justine, 3175 Chemin de la Côte-Sainte-Catherine, Montréal, QC, Canada, H3T-1C5, Tel: +1-514-345-4931 (4482); E-mail: roch.maurice.hsj@ssss.gouv.qc.ca

Submitted: 23 November 2016; **Approved:** 02 February 2017; **Published:** 06 February 2017

Citation this article: Maurice RL, Chen KYH, Burgner D, Cheung M, Vaujois L, et al. Characteristics of Arterial Wall Stiffness in Healthy Adolescents: Preliminary Mechanical Mapping of the Main Upper Body Arterial Branches. Adv J Vasc Med. 2017;2(1): 001-005.

ABSTRACT

Background: Arterial stiffness is an independent predictor of cardiovascular disease. Independent of aging and other cardiovascular risk factors, arterial stiffness increases from the proximal to the distal arterial compartments. The overall aim of this work is to establish a longitudinal mechanical mapping of the arterial tree in healthy individuals.

Methods: We report preliminary data quantifying stiffness of the abdominal aorta (AAA), common carotid artery (CCA) and brachial artery (BA) in adolescents. In group-1 subjects (from Melbourne, Australia), cine-loops of the AAA and CCA B-mode data were digitally recorded, whereas in group-2 (from Montreal, Canada), cine-loops of the CCA and BA B-mode data were acquired at the same clinical evaluation. Arterial wall elastic moduli (E_{IBM}) were estimated off-line using our proprietary non-invasive imaging-based biomarker algorithm (ImBioMark).

Results: Group-1 (n = 13) was 12.9 ± 2.5 years, with normal body habitus, blood pressure 117 ± 6 / 64 ± 4 mmHg and heart rate 71 ± 12 beats/min. Group-2 (n = 11) was 14.4 ± 1.2 years, also with normal body habitus, blood pressure 112 ± 10 / 64 ± 6 mmHg and heart rate 73 ± 10 beats / min. Arterial stiffness increased from proximal to distal compartments, with E_{IBM} of 31 ± 6 kPa (AAA), 49 ± 16 kPa (CCA) and 130 ± 26 kPa (BA); $p < 0.001$.

Conclusion: This paper contrasts, for the first time, stiffness between AAA, CCA and BA in the same adolescents. Further investigations will include additional arterial beds (pulmonary, renal and femoral) and will increase sample size to allow age-stratification. The current preliminary findings indicate that longitudinal mechanical mapping of the arterial tree in healthy individuals is feasible.

Keywords: Arterial wall stiffness; Arterial tree; Abdominal aorta; Common carotid artery; Brachial artery; Cardiovascular disease; Ultrasound elastography; Imaging-based biomarker (*ImBioMark*)

INTRODUCTION

The arterial wall is made up of the intima, media and adventitia layers. The media, mostly consisting of lamellae of elastic material, layers of vascular smooth muscle cells, and collagen fibers, is largely responsible for arterial compliance [1]. Collagen, which is at least two orders of magnitude stiffer than elastin and smooth muscle cells, predominates in peripheral arteries leading to increasing vascular stiffness from the proximal to the distal arterial compartments [2].

Arterial stiffness, which increases with age [3] and with cardiovascular risk factors [4], is an independent predictor of cardiovascular disease. Non-invasive vascular ultrasound elastography (NIVE) has been proposed as a method to quantify stiffness in superficial arteries [5-7]. Although those previous applications used radiofrequency data, NIVE has been adapted to process B-mode images; in this context it is referred to as ImBioMark (imaging-based biomarker) [8]. For the reference, we adapted ImBioMark to evaluate the ascending aortic wall remodeling in adolescents afflicted with Kawasaki disease [9] and to investigate carotid health status in adolescents born with intrauterine growth restriction [10].

Whereas the increase of arterial stiffness from proximal to distal sites, in healthy conditions, is now widely accepted, until recently no quantitative data have been reported for different arterial sites in the same subjects during the same clinical evaluation. We recently reported data contrasting the common carotid artery (CCA) and brachial artery (BA) stiffness in healthy adolescents [11]. Here we expand on this work, contrasting stiffness in the abdominal aorta (AAA), CCA and BA in healthy adolescents. The aims of the current study are to compare data obtained in two different groups of healthy subjects and to study the relative differences between distal upper body arterial stiffness and the central aorta.

METHODOLOGY

Study population

The population investigated consisted of two groups:

Group 1 (Gr-1) subjects: In Gr-1, we examined AAA and CCA in 6 male and 7 female healthy adolescents, 12.9 ± 2.5 years old, who were recruited as control subjects for a research study evaluating vascular health following Kawasaki Disease (KD). Control subjects were recruited from the outpatient clinics of The Royal Children's Hospital Melbourne, and from children of staff members and friends of KD patients. Exclusion criteria were pregnancy, diabetes, known atherosclerotic cardiovascular diseases, treatment for hypertension and/or hyperlipidaemia, or chronic inflammatory conditions requiring previous or ongoing treatment. The study was approved by the Royal Children's Hospital human research ethics committee and written consent was obtained from the parents.

After a minimum 6 hour fast, participants attended Murdoch Childrens Research Institute for a one-time appointment at which anthropometric and adiposity measurements (BC 418, Tanita, Tokyo, Japan), automated blood pressure (sphygmocor® XCEL, atcor Medical Pty Ltd, NSW, Australia), fasting lipid profile and blood glucose (Vitros 5600, Ortho-Clinical Diagnostics, Rochester, New York), and high sensitivity C-reactive protein (CRP Vario, Abbott Laboratories Inc, Abbott Park, Illinois) were obtained.

B-mode ultrasound images of the right CCA (Figure 1a) and the AAA (Figure 1b) were obtained using Vivid-i ultrasound machine (General Electronics Medical Systems, Tirat Harcarmel, Israel) with an 8 MHz linear probe and continuous electrocardiography gating. 5 to 15 cardiac cycles consisting of longitudinal images of the right CCA 1 cm proximal to the carotid bulb, and of the AAA just proximal to the femoral bifurcation were recorded for off-line analysis. The carotid artery was generally recorded at a depth of 4 cm with a frame rate of 27 images per second and the focus positioned in the middle of the artery. There were more variations in the depth of image acquisition for the abdominal aorta due to body habitus. The depth varied between 4 to 8 cm and frame rates from 14 to 27 images per second.

Group 2 (Gr-2) subjects: As previously reported [11], we examined, in Gr-2, CCA and BA in 7 male and 4 female healthy adolescents, 14.4 ± 1.2 years old, who were recruited as control subjects for a clinical research study involving children with intrauterine growth restriction, conducted at the CHU Sainte Justine. Study subjects were assessed at age thirteen to fifteen years

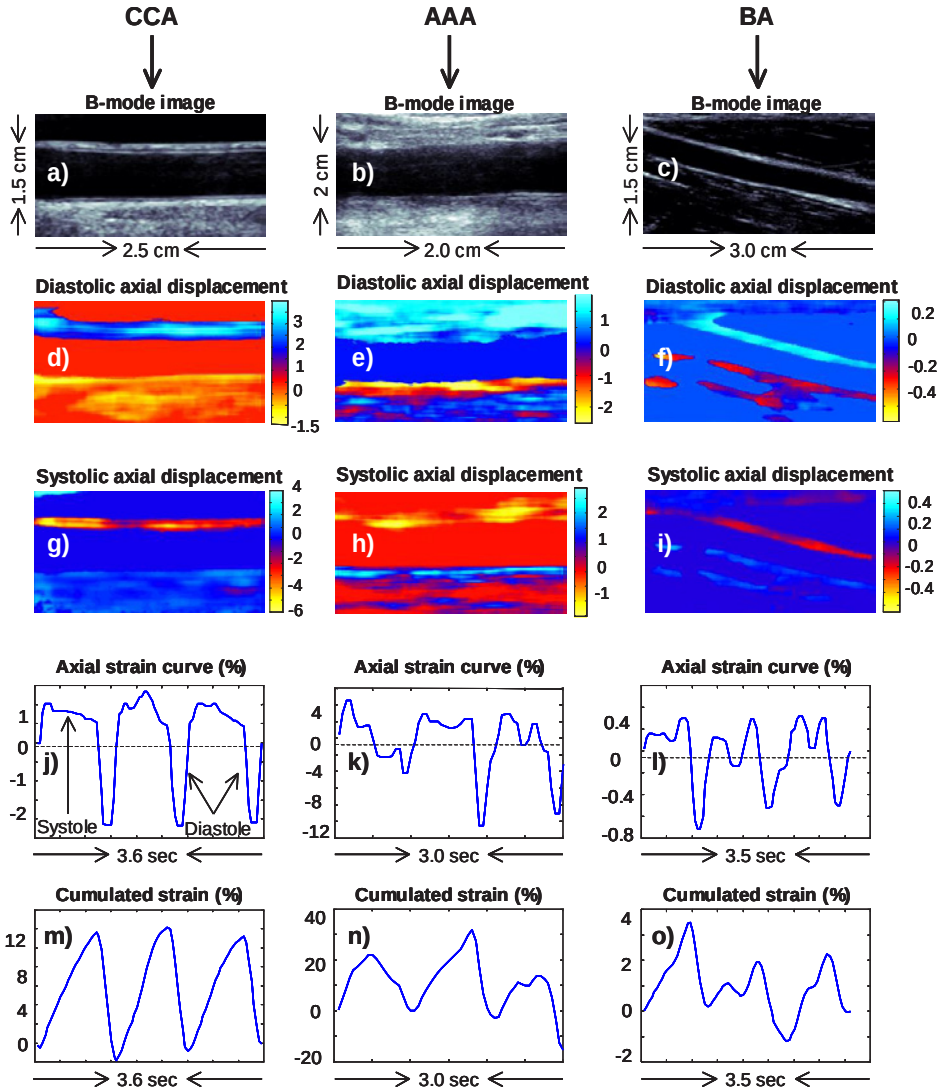

Figure 1: a-c) B-mode images of the CCA, AAA and BA, respectively
d-f) Diastolic axial displacement elastograms computed with ImBioMark for the CCA, AAA and BA, respectively; the color bar quantifies the displacement in pixels
g-i) Systolic axial displacement elastograms computed with ImBioMark for the CCA, AAA and BA, respectively; the color bar quantifies the displacement in pixels
j-l) Instantaneous axial strain curves (for 3 consecutive cardiac cycles) computed with ImBioMark for the CCA, AAA and BA, respectively
m-o) Cumulative strain curves computed with ImBioMark for the CCA, AAA and BA, respectively.

old according to a standardized protocol; they all were free of known cardiovascular co-morbidities or known cardiovascular risk factors. Cardiovascular ultrasound, blood pressure, weight and height, were obtained. The institutional ethics committee approved the study and written informed consent was obtained from the subjects' parents for this investigation.

Blood pressure was measured with an automated sphygmomanometer (Welch Allyn Inc., Skaneateles Falls, NY) prior to vascular ultrasound imaging recording. B-mode data of longitudinal segments of the right CCA and the right-arm BA (Figure c) were recorded with an iE33 Philips (Philips, Andover, Massachusetts) echography machine, using an 11 MHz probe. The frame rate was generally close to 40 Hz depending on the depth, which was typically 4 cm with the focus positioning in the middle of the artery. Loops of 7 to 8 beats were recorded serially. Electrocardiography (ECG) signals were simultaneously recorded for appropriate cardiac cycle determination as well as proper identification of systole and diastole.

ImBioMark elastic modulus calculation (E_{IBM})

ImBioMark has been described previously [8-10,12]. Briefly, the technique allows assessment of the 2D-strain tensor (Δ) as well as the 2D-displacement field (∂). Here we report data of the axial strain (Δ_{yy}) to quantify arterial wall stiffness and data for the axial displacement(∂_y) for qualitative illustration purposes. In the context of the CCA and BA, Δ_{yy} and ∂_y were computed for each pair of {n , n + 5} B-mode images, i.e. from the *speckle* changes observed between images 1 and 6, 2 and 7, etc. In the context of AAA, Δ_{yy} and ∂_y were computed for each pair of {n , n + 2} B-mode images, i.e. from the *speckle* changes observed between images 1 and 3, 2 and 4, etc. In either case, the measurement windows were set at 20 × 60 pixels, with 90% and 95% axial and lateral overlaps, respectively. Although axial strain and displacement elastograms usually were computed for 5 to 8 beats, we typically analyzed a minimum of 3 consecutive cardiac cycles per subject.

Ophir et al. [13] defined strain distribution images as strain elastograms. By extension, displacement distribution images are known as displacement elastograms. Only for qualitative illustration purposes, we present, diastolic axial displacement elastograms for the CCA, AAA and BA, in (Figures 1d-f), respectively. Equivalently, we present, in (Figures 1g-i), systolic axial displacement elastograms for the CCA, AAA and BA, respectively. In this configuration, positive displacement values (in a blue color bar) indicate downward wall motion and inversely for negative displacement values (in red/yellow color bar). Strain was assessed, at the bottom wall, in longitudinal segments typically > 1 cm length. In this context, Δ_{yy} was averaged over 3-pixel wall thickness starting from the blood / intima interface through the adventitia as a rough approximation of the intima-media thickness (IMT).

For quantitative illustration purposes, (Figures 1j-l) exhibit instantaneous strain curves computed over 3 consecutive cardiac cycles for the CCA, AAA and BA, respectively. The systolic phase of the cardiac cycle is associated with positive strain values and inversely for diastole. In addition, (Figures 1m-o) exhibit cumulative strain curves for the CCA, AAA and BA, respectively.

In the context of this study, we averaged cumulated systolic ($\bar{\Delta}_{yy}^{syst}$) and cumulated diastolic ($\bar{\Delta}_{yy}^{diast}$) strains, respectively, over at least three cardiac cycles. $\bar{\Delta}_{yy}$ was calculated as the average in absolute values of $\bar{\Delta}_{yy}^{syst}$ and $\bar{\Delta}_{yy}^{diast}$. ImBioMark elastic moduli ($\mathbf{E}_{IBM}$), for a given subject's CCA, AAA and BA, were calculated as the ratio between the pulse pressure (ΔP = peak-systole blood pressure – nadir-diastole blood pressure) and $\bar{\Delta}_{yy}$, as given in Equation 1. Based on current clinical practices, ΔP refers to brachial artery pulse pressures.

$$E_{IBM} = \frac{\Delta P}{\bar{\Delta}_{yy}}. \quad (1)$$

RESULTS

Somatic and physiological data comparisons

Somatic and physiological data are reported in (Table 1). In summary, Gr-1 subjects were 12.9 ± 2.5 years old, with normal somatic and physiological parameters. Gr-2 subjects were, on average, older (14.4 ± 1.2 years old) but with no significant statistical difference in age with Gr-1. Accordingly, Gr-2 subjects were, on average, heavier (59 ± 13 vs. 48 ± 11 kg) and taller (164 ± 9 vs. 155 ± 14 cm), but with no significant statistical difference. In addition, SBP (117 ± 6 vs. 112 ± 11 mmHg), DBP (64 ± 4 vs. 64 ± 6 mmHg) and HR (71 ± 12 vs. 73 ± 10 beats / min) were similar between Gr-1 and Gr-2.

Arterial stiffness data comparisons

The Student t-test was used for comparisons. Initially we compared carotid artery data between groups. As shown in (Table 2), carotid wall stiffness was statistically similar between Gr-1 and Gr-2 (48 ± 17 vs. 50 ± 15 kPa, respectively). Subsequently data from both groups were pooled to provide preliminary mechanical mapping of the AAA, CCA and BA (Table 3). In summary, the BA (130 ± 26 kPa) was stiffer than CCA (49 ± 16 kPa), which in turn was stiffer than AAA (31 ± 6 kPa); $p < 0.001$.

DISCUSSION

An accurate assessment of arterial stiffness may help early detection of vascular diseases as well as stratifying the amplitude of the disease affecting the vessels. Whereas intima-media thickness was developed to measure anatomical changes to the carotid arteries,

Table 1: Somatic and physiological parameters.

Parameters	Mean ± Std		p
	Group-1	Group-2	
Count	13	11	
Males / females	6 / 7	7 / 4	
Age (years)	12.87± 2.51	14.45 ± 1.17	0.068
Weight (kilograms)	48 ± 11	59 ± 13	0.068
Height (cm)	155 ± 14	164 ± 9	0.059
Systolic blood pressure (mmHg)	117 ± 6	112 ± 11	0.258
Diastolic blood pressure (mmHg)	64 ± 4	64 ± 6	0.771
Pulse pressure (mmHg)	53 ± 9	49 ± 9	0.284
Heart rate (beats/min)	71 ± 12	73 ± 10	0.696

Table 2: Comparison of CCA stiffness between Gr-1 and Gr-2.

Population	n	Males / females	Mean ± Std (kPa)	*p*
Group-1	13	6 / 7	48 ± 17	0.86
Group-2	11	7 / 4	50 ± 15	

Table 3: Comparison of arterial stiffness in proximal and distal arteries.

Artery	Count	Males / females	Mean ± Std (kPa)	*p*
Abdominal aorta	13	6 / 7	31 ± 6	< 0.001
Common carotid	24	13 / 11	49 ± 16	
Brachial	11	7 / 4	130 ± 26	

ImBioMark measures dynamic response of the arterial vascular wall to distension and recoil forces as they are generated throughout systole and diastole. In this perspective, our assessment is unique and gives a new functional perspective of the arterial wall structure. It is worth noting that ImBioMark was designed to assess mechanical properties of large and medium size vessels that are transcutaneously accessible; namely the carotid, abdominal aorta and brachial arteries in this study. The algorithm is applicable to clinically available ultrasound imaging modalities; namely DICOM format data recorded with a Vivid-i and an iE33 Philips ultrasound machines in the current investigation.

In the present study, we aimed to compare the arterial stiffness of the AAA, CCA and BA in healthy adolescents. Distal arteries were stiffer than proximal arteries; in keeping with the predominance of collagen over elastic in peripheral arteries [2]. Here we show for the first time, in an adolescent population, the progressive increase of stiffness from AAA to CCA and BA. This work adds to our previous findings [11] and is an additional step toward extensive vascular mapping of arterial wall elastic properties. In summary, the mechanical mapping of the main upper body arterial branches for healthy adolescents (around 13 years old) would be: AAA (31 ± 6 kPa), CCA (49 ± 16 kPa) and BA (130 ± 26 kPa). We are investigating a larger cohort of healthy subjects as to allow age-stratification and to include additional arteries such as the pulmonary, the renal and the femoral.

We have compared carotid artery's stiffness between Australian and Canadian adolescents. Although additional data are required to confirm the observations of the current study, we intend, in a long-term perspective, to investigate the interrelationships of cardiovascular disease with genetic and environmental predispositions.

Comparison with PWV

Pulse wave velocity (PWV) is an established measure of arterial stiffness, proving to be an important predictor of cardiovascular events [14]. Looking at the literature, Jo et al. found thoracic aortic PWV of 3.04 m/s for a population aged 0 to 20 years [15], although Fulton and McSwiney measured 4.2 m/s brachial PWV for children and adolescents (5 to 15 years old) [16]. In addition, Munoz-Tsorrero et al. assessed brachial PWV of 7.96 m / s for adults (> 30 years old) [17] and Blacher et al. 12.4 m / s for adults (> 40 years old) [18]. In summary, these results likely pointed out 1) An increase in stiffness with age of the brachial artery, and 2) An increase in stiffness of the arteries from proximal to distal sites, in concordance with our results.

Potential limitations of ImBioMark

We recently discussed the difficulties and potential solutions associated with imaging BA [11]. In the current study, the deviations of the BA B-mode images from the horizontal plane were less than 30 degrees. According to [19] there was then no need to compensate for bias in motion estimates. We also modeled the motion artifacts that can be induced by the complex dynamics of the aorta artery [9]. In the context of this investigation, the aortic data exhibited reasonably good quality. Although it was not of concern here, we may need to implement the angle compensation method for BA and likely a segmentation algorithm for the aorta to improve ImBioMark potential to investigate large subject cohorts from worldwide.

In the context of the CCA and BA, mechanical parameters (Δ_{yy} and ∂_y) were computed for each pair of {n , n + 5} B-mode images. For AAA, Δ_{yy} and ∂_y were computed for each pair of {n , n + 2} B-mode images. The smaller the step the more correlated are the images to be analyzed, which is more appropriate to assess the complex dynamics of the aorta artery wall. It is worth noting that the step does not bias the stiffness measurement, since strain cumulated over several cardiac cycles (≥ 3) was typically used to calculate the elastic moduli (Equation 1).

Depending on the depth, the frame rate used to record the aorta data cine-loops was typically less than that for the carotid and brachial arteries. Similar to the step, this parameter does not bias the stiffness measurement. Nevertheless, under the 15 Hz frame rate, *ImBioMark* may become unreliable because of *speckle* decorrelation originated from large motion of the aortic wall.

The systolic phases associated with (Figures 1m, 1n and 1p) seem to indicate a linear behaviour of arterial wall, suggesting that we are assessing an intrinsic mechanical property of the arteries, i.e. the Young's modulus. Nevertheless, further data are required to confirm this hypothesis.

Finally, it is important to note that, in current clinical applications, only brachial measurements of arterial blood pressures are achievable. This is the rationale supporting the use of the brachial pulse pressure (ΔP) to compute the elastic moduli (Equation 1). Given the differences in pulse pressures between central and peripheral arterial sites, this potentially may induce biases in the aortic and carotid elastic moduli estimations.

CONCLUSION

This paper contrasts, for the first time, stiffness between the abdominal aorta, common carotid and brachial arteries in the same adolescent subjects, with increasing stiffness in distal compared to proximal arteries. These findings suggest that longitudinal mechanical mapping of the arterial tree in healthy individuals is feasible. In the longer term, these findings may facilitate identification of those at increased risk of cardiovascular disease earlier in the life course, thereby allowing primary and primordial prevention, prior to the onset of clinical disease.

REFERENCES

1. Benetos A, Bouaziz H, Albaladejo P, Guez D, Safar ME. Carotid artery mechanical properties of Dahl salt-sensitive rats. Hypertension. 1995; 25: 272-277.
2. Li, John K-J. The arterial circulation: physical principles and clinical applications. Totowa: Human Press. 2000; 271.
3. Benetos A, Waeber B, Izzo J, Mitchell G, Resnick L, Asmar R, et al. Influence of age, risk factors, and cardiovascular and renal disease on arterial stiffness: Clinical applications. American Journal of Hypertension. 2002; 15: 1101-1108.
4. Liao J, Farmer J. Arterial Stiffness as a Risk Factor for Coronary Artery Disease. Current Atherosclerosis Reports. 2014; 16: 387.
5. Mai JJ, Insana MF. Strain imaging of internal deformation. Ultrasound in medicine and biology. 2002; 28: 1475-1484.
6. Maurice RL, Ohayon J, Frétigny Y, Bertrand M, Soulez G, Cloutier G. Non-invasive Vascular Elastography : Theoretical Framework. IEEE Transactions on Medical Imaging. 2004; 23: 164-180.
7. Maurice RL, Soulez G, Giroux MF, Cloutier G. Non-invasive vascular elastography for carotid artery characterization on subjects without previous history of atherosclerosis. Medical physics. 2008; 35: 3436-3443.
8. Maurice RL, Dahdah N, Tremblay J. Imaging-based Biomarkers: Characterization of post-Kawasaki Vacuities in Infants and Hypertension Phenotype in Rat Model. International Journal of Vascular Medicine. 2012; 2012: 364145.
9. Maurice RL, Dahdah N. Characterization of aortic remodeling following Kawasaki disease: Toward a fully-developed automatic bi-parametric model. Medical Physics. 2012; 39: 6104-6110.
10. Maurice RL, Vaujois L, Dahdah N, Chibab N, Maurice A, Nuyt AM, et al. Carotid wall elastography to assess midterm vascular dysfunction secondary to intrauterine growth restriction: Feasibility and comparison with standardized intima-media thickness. Ultrasound in Med Biol. 2014; 40: 864–870.
11. Maurice RL, Vaujois L, Dahdah N, Nuyt AM, Bigras JL. Comparing carotid and brachial artery stiffness: a first step toward mechanical mapping of the arterial tree. Ultrasound in Med Biol. 2015; 41: 1808–1813.
12. Zakaria T, Qin Z, Maurice RL. Optical Flow-based B-Mode Elastography: Application in Hypertensive Rat Carotid. IEEE Transactions on Medical Imaging. 2010; 29: 570-578.
13. Ophir J, Céspedes I, Ponnekanti H, Yazdi Y, Li X. Elastography: A quantitative method for imaging the elasticity of biological tissues. Ultrasonic Imaging. 1991; 13: 111-134.
14. Laurent S, Cockcroft J, Van Bortel L, Boutouyrie P, Giannattasio C, Hayoz D, et al. Expert consensus document on arterial stiffness: methodological issues and clinical applications. Eur. Heart J. 2006; 27: 2588-2605.
15. Jo CO, Lande MB, Meagher CC, Wang H, Vermilion RP. A simple method of measuring thoracic aortic pulse wave velocity in children: methods and normal values. J Am Soc Echocardiogr. 2010; 23: 735-740.
16. Fulton JS, MaSwiney BA. The pulse wave velocity and extensibility of the brachial and radial artery in man. J Physiol. 1930; 69: 386–392.
17. Munoz-Tsorrero JF, Tardio-Fernandez M, Valverde-Valverde JM, Duque-Carrillo F, Vega-Fernandez JM, Joya-Vazquez P, et al. Pulse Wave Velocity in Four Extremities for Assessing Cardiovascular Risk Using a New Device. The Journal of Clinical Hypertension. 2014; 16: 378-384.
18. Blacher J, Asmar R, Djane S, London GM, Safar ME. Aortic Pulse Wave Velocity as a Marker of Cardiovascular Risk in Hypertensive Patients. Hypertension. 1999; 33: 1111-1117.
19. Mercure É, Deprez JF, Fromageau J, Basset O, Soulez G, Cloutier G, et al. A compensative model for angle-dependence of motion estimates in Non-Invasive Vascular Elastography. Medical Physics. 2011; 38: 727-735.